# Development and Characterization of PLA nanoparticles for pulmonary drug delivery: Co-encapsulation of theophylline and budesonide, a hydrophilic and lipophilic drug

*Mira Dhiraj Buhecha*[a], *Alison B. Lansley*[a], *Satyanarayana Somavarapu*[b], *Ananth S. Pannala*[a,*]

[a] Biomaterials & Drug Delivery Research Group, School of Pharmacy and Biomolecular Sciences, University of Brighton, Lewes Road, Brighton, BN2 4GJ, UK

[b] UCL School of Pharmacy, 29-39 Brunswick Square, London, WC1N 1AX, UK

***Corresponding Author:**
Dr. Ananth S. Pannala FRSC
School of Pharmacy and Biomolecular Sciences
University of Brighton
Lewes Road
Brighton – BN2 4GJ
UK
Email: a.s.v.pannala@brighton.ac.uk
Tel: +44 1273 642 109
Fax: +44 1273 642 674

**Abstract**

Drug encapsulated biodegradable polymeric nanoparticles are suitable for lung delivery of therapeutic molecules. The objective of the current study was to co-encapsulate a hydrophilic drug (theophylline) and a lipophilic drug (budesonide) in poly(lactic acid) (PLA) nanoparticles for pulmonary drug delivery. PLA nanoparticles were produced using a double emulsification solvent diffusion method and characterized for their particle size, zeta potential, drug loading, *in vitro* drug release, interactions with airway epithelial cell line (16HBE14o-) and *in vitro* deposition properties upon nebulization. The spherically-shaped mono- and co-encapsulated PLA nanoparticles were observed to have a particle size of 190–400nm and a zeta potential of –10 to –16mV. Sustained drug release over 24h was observed from the nanoparticles into a mixture of simulated lung fluid and methanol (1:1), measured using Franz diffusion cells and when assessed for permeability using 16HBE14o- cells. There was no significant reduction in cell viability after 24h exposure to drug-encapsulated nanoparticles at nebulized concentrations ($p>0.05$). Nebulization of co-encapsulated nanoparticles resulted in a fine particle fraction of 75% and 48% for theophylline and budesonide, respectively. From these observations it can be concluded that budesonide and theophylline drug-loaded PLA nanoparticles are suitable drug delivery systems for combination therapy of asthma and COPD.

*Keywords:* Theophylline; Budesonide; Franz diffusion cells; Poly(lactic acid); co-encapsulation; nanoparticles; 16HBE14o- cells

## 1. Introduction

Various polymers, synthetic and natural, have been used to produce nanoparticles for several drug delivery applications. A number of studies have shown that biodegradable polymers can be used in the preparation of nanoparticles for encapsulating mostly lipophilic drugs thereby allowing for an extended drug release profile [1,2,3,4]. Examples of such polymers include synthetic polyesters: poly(DL-lactic acid) (PLA), poly(lactic-co-glycolic acid) (PLGA) and polyacrylates such as poly(ε-caprolactone) (PCL) and naturally-occurring biodegradable polymers such as chitosan, albumin, gelatin and alginate [4,5,6]. Polyesters, PLA and PLGA, degrade to natural metabolites lactic acid and/or glycolic acid, which are subsequently metabolized in the body *via* the citric acid cycle and pyruvate cycle to produce non-toxic by-products such as carbon dioxide, water and nitrogen [7]. Due to the slow degradation of the polymers and the formation of natural metabolites it is believed that these polymers should not affect normal cell function [8,9].

The use of nanoparticles to deliver medications *via* the pulmonary route is an extensively researched area. For respiratory diseases such as asthma and chronic obstructive pulmonary disease (COPD) it is ideal for the drugs to be delivered directly to the site of action. Several drugs such as budesonide [10], fluticasone propionate [11], voriconazole [12], levofloxacin [13], siRNA [14], other antibiotics [15], anticancer drugs [16] and insulin [17] have been developed as potential micro- and nanoparticle formulations and tested for pulmonary drug delivery, including PLGA particles loaded with theophylline and budesonide [18] with varying degrees of success. A number of drugs used in the treatment of lung conditions are currently available as oral formulations with the most common being theophylline, mast cell

stabilizers and leukotriene antagonists. It is hypothesized that co delivery of budesonide and theophylline enhances the therapeutic effect.

The current study focused on the development of a unique method to produce PLA nanoparticles co-encapsulated with budesonide (a model lipid-soluble drug) and theophylline (a model water-soluble drug). Budesonide is a commonly prescribed inhaled corticosteroid used for the treatment of asthma and COPD. It is a 16,17 acetal series, non-halogenated potent glucocorticoid which, by inhalation, has predominantly local effects on the lungs. Budesonide has a Log P of 2.17, allowing rapid uptake into the airway mucosa. Currently, budesonide is available as a dry powder inhaler, pressurized metered dose inhaler and nebulizer inhalation formulation and in combination with formoterol fumarate (long acting β2-agonist).

Theophylline is a potent bronchodilator and is commonly prescribed, *via* the oral route, as an additive medication in the later stages of the treatment of asthma in combination with a short acting β2-agonist, long acting β2 agonist or an inhaled corticosteroid. However, due to theophylline's narrow therapeutic range of 30-100 µM and adverse effects at concentrations greater than 110 µM, it has an increased risk of side-effects making it the third choice medication for the treatment of asthma. In contrast to budesonide, theophylline is a water-soluble drug with a Log P of -0.02.

Extended drug release by the use of biodegradable polymers allows for a reduced frequency of dosing thereby potentially increasing patient compliance [19]. Nanoparticles in general are expected to have a longer residence time in circulation and in tissues leading to a longer duration of localized action and would also facilitate in increasing the half-life of the nanoparticles and improving their overall bioavailability [20,21]. This would result in a better control of symptoms over a longer

period of time. The purpose of this study, was to develop a method to successfully co-encapsulate both hydrophilic theophylline and the lipophilic budesonide using PLA as the encapsulating polymer. The aim was to produce a preparation exhibiting sustained release of both drugs to enable the dosing interval to be extended and patient adherence to be increased. A double emulsification solvent diffusion (DESD) method was developed to produce budesonide and theophylline co-encapsulated PLA nanoparticles which were characterized for particle size, zeta potential, surface characteristics, morphology, loading efficiency, drug release, using Franz diffusion cells, and *in vitro* deposition properties upon nebulization using a multi-stage liquid impinger (MSLI). The nanoparticles produced were also assessed for cellular toxicity and transport of the drugs across an *in vitro* model of the airway epithelium using the 16HBE14o- cell line. Mono-encapsulated drug-PLA nanoparticles were also prepared and characterized for comparison with the co-encapsulated drug-PLA nanoparticles.

## 2. Materials and methods

### 2.1. Materials

Poly (lactic acid) (PLA) (Purasorb® PDL02; molecular weight – 17,000 kda) was purchased from Purac Biomaterials, Netherlands. Poly (vinyl alcohol) (PVA) (molecular weight – 15,000), theophylline (>99% anhydrous powder), Dimethylsulfoxide (DMSO) and 3-(4,5-dimethyl-2-thiazolyl)-2,5-diphenyl-2H-tetrazolium bromide (MTT) were purchased from Sigma Aldrich, UK. Budesonide was purchased from LKT Laboratories, USA. Trypan blue stain (0.4% w/v) was purchased from Life Technologies, USA. All other chemicals and solvents were of laboratory and HPLC grade. Cellulose membrane (dialysis visking tubing) was purchased from Medicell Membranes, Liverpool, UK. Reagents and materials used for cell culture were purchased from Fisher Scientific Ltd. (Loughborough, UK) unless specified otherwise. 16HBE14o- cells were a kind gift from Professor Dieter Gruenert formerly of University of California, San Francisco, USA.

### 2.2. Preparation of PLA nanoparticles

Nanoparticles were prepared at a weight/weight ratio of 1:4 for mono-encapsulated theophylline–PLA nanoparticles, 1:40 ratio for mono-encapsulated budesonide–PLA nanoparticles and 10:1:40 ratio of theophylline-budesonide-PLA for the co-encapsulated nanoparticles. Mono- and co-encapsulated PLA nanoparticles were prepared using a modified DESD method [4]. Nanoparticle preparation parameters are shown in Table 1. Briefly, the co-encapsulated nanoparticles were prepared by dissolving PLA and budesonide in 10 ml of dichloromethane (DCM) and theophylline was dissolved in 10 ml of 2% w/v PVA solution. The organic and aqueous solutions were homogenized at 10,000 rpm (IKA®-25 Digital Ultra Turrax

Homogeniser, UK) and 10 ml of acetone was added to the mixture while homogenizing (total duration 5 min). Acetonitrile and ethyl acetate were also investigated as alternative solvents to acetone (Table 1). The novel approach of using a second water-miscible organic solvent, acetone, helped in the encapsulation of the hydrophilic drug (theophylline) as it allowed the drug to partition across the organic and aqueous phase. The resultant emulsion was added drop wise to an excess of aqueous phase (100 ml of 18.2 MΩ deionized water) and further homogenized to destabilize the initial emulsion. The organic solvents in the emulsion were then evaporated by rotary evaporation (IKA®RV-10 control with water bath and Vacuubrand chemistry diaphragm pump, UK) at 70 mbar and 130 rpm until all the organic solvent was removed. The resultant suspension of PLA nanoparticles was centrifuged at 15,000 rpm (25,000 *g*) for 15 min (at 4°C) (Sorvall RC-6 Plus™ Superspeed centrifuge, Loughborough, UK)). The supernatant was transferred into another container and the pellet was re-suspended in 2 ml of 18.2 MΩ deionized water. The samples were then freeze-dried (Alpha 2-4 freeze drier, Martin Christ, Germany) for 24 h to yield encapsulated PLA nanoparticles. The freeze-dried samples were stored at room temperature until further characterization and analysis.

Mono-encapsulated nanoparticles were prepared in an identical manner to co-encapsulated nanoparticles but by avoiding either budesonide or theophylline in the initial emulsion preparation. Blank nanoparticles were also prepared in an identical manner by using only the PLA (organic) and PVA (aqueous) solutions. All the remaining steps in the preparation of nanoparticles were identical to the ones used for the preparation of co-encapsulated nanoparticles. All the nanoparticle samples, *viz*. blank nanoparticles, mono-encapsulated nanoparticles and co-encapsulated nanoparticles, were prepared in triplicate.

### 2.3. Determination of nanoparticle morphology

Particle size distribution and surface morphology of the nanoparticles were investigated by scanning electron microscopy (SEM) using a field emission gun scanning electron microscope (FEG-SEM) (Zeiss SIGMA, Japan). Freeze dried samples were prepared on aluminum stubs and coated with platinum with a thickness of 4-5 nm (Q150T Turbo-pumped sputter coater, Quorum technologies, UK). The samples were placed in the SEM chamber and scanned at a voltage of 2 kV and working distance of 4-10 mm.

### 2.4. Analysis of nanoparticle surface characteristics using Fourier Transform Infra-red (FT-IR) spectroscopy

The surface characteristics of the nanoparticles were investigated on a Perkin Elmer Spectrum 65 Infra-red spectrophotometer with a Universal ATR sampling assessor (UK). Drug and polymer standards were obtained and compared to all the freeze-dried nanoparticle samples. A scanning range of 400 – 4000 $cm^{-1}$ was selected and a resolution of 4 $cm^{-1}$.

### 2.5. Determination of particle size and surface charge

The particle size and charge of the different freeze-dried nanoparticles was determined by photon correlation spectroscopy (PCS) (Malvern Zetasizer Nanoseries, Nano-ZS690 Malvern Instruments, UK). An accurately weighed amount (1- 3 mg) of the freeze dried nanoparticle sample was suspended in 10 ml of 18.2 MΩ deionized water and vortex mixed for 30 seconds. For particle size analysis, the sample was then transferred to a plastic disposable cuvette and placed in the

Zetasizer. For zeta potential measurements, samples were transferred to folded capillary cuvettes, with gold plated electrodes. Analysis was carried out at 25°C and each measurement was carried out in triplicate.

### 2.6. Thermal analysis of nanoparticles

Thermal analysis of the nanoparticles was studied using a differential scanning calorimeter (DSC) (Mettler Toledo StarE software, UK). An accurately weighed amount (2 mg) of the freeze dried nanoparticle powder or drug and polymer standards or a physical mixture of the polymer (200 mg PLA) and drugs (5 mg budesonide and 50 mg theophylline) were weighed into each DSC aluminum pan. The pan was then crimp-sealed, the lid was pierced and the pan placed in the DSC. An empty sealed aluminum pan with pierced lid was used as a reference. Each sample was analyzed over the temperature range of 25–400°C at a heating rate of 10°C/min to determine the melting temperatures of the drugs, polymer and nanoparticles.

### 2.7. Determination of drug loading efficiency in the nanoparticles

High performance liquid chromatography (HPLC) was used to determine the loading efficiency of theophylline and budesonide in the mono- and co-encapsulated nanoparticles. The samples were analyzed using a Fortis C18 column (4.6x150 mm, 5 µm particle size, Fortis Technologies Ltd, UK) on a HPLC system which consisted of a HP1050 Pump system, autosampler and UV-Vis detector (Hewlett Packard, USA) using TotalChrom Navigator-900 Software. The mobile phase consisted of methanol (70%) and water (30%), at a flow rate of 1 ml/min at 25°C with a detector wavelength of 260 nm. Standard concentrations of both the drugs over the range of

0.1–20 µg/ml were prepared in methanol in triplicate and calibration graphs were plotted. A linear response with a correlation coefficient value of $R^2 \geq 0.999$ was obtained over the entire calibration range for both theophylline and budesonide.

In order to determine the loading efficiency of drug-loaded nanoparticles, accurately weighed freeze dried nanoparticles were suspended in 3 ml of methanol and placed in an ultrasonic bath for 1 h. The samples were then left at room temperature for 24 h followed by centrifugation (Eppendorf Minispin Microfuge, UK) at 14,000 rpm for 20 min. An aliquot of 1 ml of the clear supernatant was transferred into a HPLC vial and analyzed. Loading efficiency was calculated as described by Li et al. [22].

### 2.8. *In vitro* drug release from the nanoparticles

*In vitro* drug release of theophylline and budesonide from mono- and co-encapsulated PLA nanoparticles into a simulated lung fluid (SLF)–methanol mixture (1:1) was determined using Franz diffusion cells. An inert synthetic cellulose membrane (pore size: 24 Å (Medicell Membranes, Liverpool, UK)) was mounted between the donor and receiver chamber of the Franz diffusion cell and the receiver chamber was filled with 50:50 SLF–methanol (2 ml, receiver fluid). SLF was chosen to represent the medium found in the airways to which the nanoparticles would be delivered. Methanol was included as a co-solvent in order to facilitate drug release as well as for analyzing the drug concentration. SLF solution was prepared as described by Marques et al [23]. Mono- or co-encapsulated freeze-dried nanoparticles (3 mg) were suspended in 5 ml of SLF and vortex mixed thoroughly. An aliquot of 0.5 ml of the suspension was transferred to the donor chamber. The Franz diffusion cell was then incubated at room temperature for a total duration of 24

h. Aliquots of the receiver fluid (0.2 ml) were removed and replaced with fresh receiver fluid at regular time points. Throughout the experiment, any loss of receiver fluid due to evaporation from the Franz cell was replaced to maintain a constant volume. The samples were analyzed by HPLC as described in section 2.7 and the amount of theophylline and budesonide that had permeated through the membrane over the incubation period was calculated using appropriate calibration graphs constructed in the receiver fluid. Drug solutions were prepared in SLF at concentrations equivalent to those present in the nanoparticles (116 µg/ml theophylline and 23.52 µg/ml budesonide) to allow comparison of permeability of encapsulated and free drugs over a period of 24 h.

## 2.9. Characterization of nanoparticles using a human bronchial epithelial cell line

### 2.9.1. 16HBE14o- cell culture

16HBE14o- cells (passage number 69 – 122) were routinely cultured in Minimal Essential Medium (MEM) supplemented with 10% (v/v) fetal bovine serum (FBS) supplemented with penicillin (100 units/ml) /streptomycin (100 µg/ml) solution (cell culture medium I). Cells were maintained at 37°C in a humidified atmosphere of 95% air and 5 % $CO_2$.

### 2.9.2. Effect of theophylline, budesonide and co-encapsulated nanoparticles on the viability of 16HBE14o- cells

The cytotoxicity of solutions of theophylline and budesonide at concentrations equivalent to those encapsulated in the nanoparticles and of the drugs co-encapsulated into nanoparticles was determined by conducting an MTT assay. Cells

were seeded at a cell density of 4000 cells/well in 96 well plates and cultured in cell culture medium I for 24 h. Nanoparticles (prepared as a suspension in cell culture medium I) were added to the wells at a concentration range of 0.25 mg/ml - 5 mg/ml (100 µL/well). Solutions of theophylline (0.05 – 1.0 mg/ml) and budesonide (5 - 100 mg/ml) were prepared in cell culture medium I. MTT solution was made to a final concentration of 5 mg/ml in MEM (without FBS and antibiotics). After incubating the cells for 24 h with the nanoparticles or drug solutions, 100 µL of MTT solution was added to each well and the cells were incubated for a further 2 h. MTT solution was then carefully aspirated from the cells and DMSO (100 µL) was added to each well. The cells were left at room temperature for 1 h and the absorbance of each well was measured at 595 nm (Multiskan Ascent, v123).

### 2.9.3. Transport of free and co-encapsulated theophylline and budesonide across 16HBE14o- cells

Polycarbonate cell culture supports (Transwell®) were coated with collagen (Purecol, Advanced Biomatrix, USA) and stored at 2-8°C for at least 24 h. After rinsing the supports with PBS, 16HBE14o- cells were seeded at 4.3 x $10^5$ cells/well and incubated at 37°C in a humidified atmosphere of 95 % air and 5% $CO_2$. After 24 h, the cell culture medium (Dulbecco's Modified Eagle's Medium (DMEM) (with L-Glutamine):Ham's F12 medium (1:1) (supplemented with 2% v/v Ultroser G® (BioSepra SA, France) and 100 U/ml penicillin/ 100 µg/ml streptomycin) (cell culture medium II)) was removed from the apical chamber, bringing the cells to an air-liquid interface. Subsequently, cells were fed basolaterally every 48 h. Cells were used seven days after seeding.

Prior to commencing drug transport study, the transepithelial electrical resistance (TER) of the cells was measured (EVOM Epithelial Tissue Voltohmmeter and 'chopstick' silver chloride electrodes (World Precision Instruments Inc., USA)). The cell culture medium was replaced with pre-warmed transport medium (DMEM (with L-glutamine):Hams F12 medium (1:1) mixture) in both the apical (1 ml) and basolateral (2 ml) chambers. The cells were incubated for 1 h at 37°C in a humidified atmosphere (95% air: 5% $CO_2$) and resistance was measured in triplicate for each well. The TER of the cell layer was calculated by subtracting the TER of a cell-free culture support measured under the same conditions.

Drug transport was measured in the apical to basolateral direction. Nanoparticle suspensions (blank (without drug), mono- and co-encapsulated) and drug solutions were prepared in transport medium. The concentration of nanoparticles applied to the cells was 0.6 mg/ml. The concentration of theophylline and budesonide applied was equivalent to the concentration encapsulated in the nanoparticles (118 and 39 µg/ml, respectively). The test solutions also contained 250 µM fluorescein-isothiocyanate (FITC)-labeled dextran (molecular weight 3,000 – 5,000) (FD4).

Samples were taken from the basolateral chamber (200 µL) at 60 min intervals up to 6 h and at 24 h. The samples were analyzed for drug content and FD4 using HPLC and fluorescence spectroscopy, respectively. FD4 concentration was measured using an excitation wavelength of 485/20 nm and emission wavelength of 528/20 nm (BioTek Gen5 microplate reader, Swindon, UK). The apparent permeability coefficient (Papp) of each compound was calculated as shown in Equation 1:

$$P_{app} = \left(\frac{dq}{dt}\right)/(A.C_0)$$ Equation 1

Where (dq/dt) is the rate of transport of the test sample, A represents the surface area of the Transwell and $C_0$ represents the initial concentration of the drug or FD4 applied to the apical chamber.

### 2.10. Deposition of nebulized nanoparticles using a multi-stage liquid impinger (MSLI)

Mono- and co-encapsulated nanoparticles were nebulized using a jet nebulizer (Omron compAIR, Omron Healthcare UK Ltd., Milton Keynes, UK) into a multi-stage liquid impinger (MSLI) (Copley Scientific Ltd, Nottingham, UK). A nanoparticle suspension for nebulization was prepared by suspending 5 mg of freeze-dried nanoparticles in 5 ml of deionized water. The samples were sonicated for 60 s followed by thorough vortex mixing for a further 2 min.

Deionized water–methanol mixture (30:70 %v/v) (20 ml) was placed in stages 1 to 4 of the MSLI and the filter stage was covered with a filter paper (76 mm diameter, pore size: 0.45 µm, Fisherbrand, UK). A suitable molded rubber mouthpiece and adapter were placed in-line along the horizontal axis of the induction port. A flow rate of 60 L/min for the MSLI was achieved using a calibrated digital flow meter (Copley Flow meter (Model: DFM3), Copley Scientific Ltd, Nottingham, UK) and a vacuum pump (Copley High Capacity Vacuum Pump (HCP5), Copley Scientific Ltd, Nottingham, UK), as recommended by the manufacturer. Nebulization was carried out for a period of 5 min at a flow rate of 0.5ml/min followed by washing the induction port, mouth piece, individual stages and filter paper with a pre-determined volume (10 ml) of methanol to extract the drugs. The MSLI itself was sealed with Parafilm®

to avoid any loss of solvent and gently shaken to dissolve the drugs from the individual stages of the apparatus. The amounts of theophylline and budesonide deposited in each stage of the MSLI as well as on the filter paper and the mouthpiece were determined by HPLC, as previously described in section 2.7. The fine particle dose (FPD) (µg) was calculated from stages 2-5 of the MSLI when in operation at 60 L/min. This was then used to calculate fine particle fraction (FPF) (%) which was obtained from FPD x 100. Emitted dose (ED) is the total amount of drug recovered from the throat and stages 1-5 of MSLI.

### 2.11. Statistical analysis

All measurements were carried out at least in triplicate and the mean ± standard deviation of all data are presented. The samples were compared statistically using a Mann-Whitney, One-way ANOVA (physico-chemical characterization) or Two-way ANOVA tests (release and aerosolization characterization). The observations were considered to be significantly different with $p$-value < 0.05 (95% probability).

## 3. Results and Discussion

### 3.1. Preparation and characterization of PLA nanoparticles for their morphology and surface characteristics (SEM and FT-IR)

Different methods, such as polymerization of the monomer, emulsion-solvent evaporation, nanoprecipitation, salting out, etc., have been described in the literature to enable encapsulation of drugs into polymeric nanoparticle systems [4]. Encapsulation of hydrophobic drugs is easier than encapsulation of hydrophilic drugs due to the latter's greater affinity for the external aqueous phase, which results in a lower loading efficiency. The DESD method employed in the current study resulted in the successful formation of nanoparticles. The novel approach of using a second water-miscible organic solvent, acetone/acetonitrile/ethyl acetate, helped in the encapsulation of the hydrophilic drug (theophylline) as it allowed the drug to partition across the organic and aqueous phase.

The method was modified and optimized in several different ways to optimize the loading efficiency of the nanoparticles. Different permutations, such as varying the: concentrations of the drug(s) and PLA; duration of homogenization to form the emulsion; evaporation procedure for the organic layer (rotary evaporation under negative pressure or simple continuous stirring); varying molecular weight (9K to 205K) and concentration (0.5% w/v to 5% w/v) of the surfactant PVA; varying the second organic solvent used, such as acetone, acetonitrile and ethyl acetate, to encapsulate the drugs, were investigated in order to produce the nanoparticles (Table 1). Surfactants such as Tween 80, Lutrol F127® and sodium dodecyl sulfate were also investigated as alternatives to PVA.

Table 1 lists the different nanoparticles attempted in the current study along with the particle size, zeta potential and loading efficiency of the two drugs, budesonide and theophylline. Methods 1-6 produced nanoparticles with large particle size variation and low levels of theophylline encapsulation. Methods 7-9 showed similar loading efficiency for both the drugs, but method 9 resulted in nanoparticles with lower zeta potential compared to methods 7 and 8. The nanoparticles produced using method 8 offered the best compromise between particle size, surface charge and loading efficiency with low variation compared to the other methods and were therefore selected for further study. All the subsequent results are shown for nanoparticles produced using this method.

Our results have shown that there was no significant advantage of using the alternative surfactants to PVA or varying the molecular weight and concentration of PVA in the preparation of nanoparticles. The observations made in this study agree with the literature that PVA is the most suitable surfactant and stabilizer for the preparation of nanoparticles [24,25].

Morphological assessment carried out by SEM revealed that these nanoparticles were spherical in shape with a smooth surface and a wide particle size distribution. Some particles exhibited a porous surface, which is likely to be an advantage for water to enter the particle leading to drug dissolution and subsequent polymer degradation. There was no difference in the morphological features of blank, mono- or co-encapsulated nanoparticles (Figure 1). The absence of drug crystals in the SEM images confirmed that any un-encapsulated drug was removed along with the surfactant in the centrifugation and washing stage of the nanoparticle synthesis. While Figure 1 shows the presence of some particles that are > 1 μm, the majority of the particles were observed to be in the nm region, as discussed subsequently.

FT-IR spectroscopy was performed to observe the surface properties and characteristics of the nanoparticles and highlight any drug adsorption. FT-IR spectra of PLA, budesonide and theophylline standards are shown in Figure 2 (A-C). The spectra and peaks present for the drug encapsulated PLA nanoparticles (Figure 2D) showed similarity to the PLA spectrum (Figure 2A). The spectra obtained showed peaks in the region of 1746.34 $cm^{-1}$, which represents the C=O ester bond of the PLA. C-O stretches are seen in the region of 1100-1400 $cm^{-1}$ for the samples. C-H bond stretches are present in the region of 2960 $cm^{-1}$ as seen for the samples. OH peaks from the background appear in the region of 3500 $cm^{-1}$. For all the samples, the resemblance of the nanoparticle FT-IR spectrum to the polymer spectrum suggests that the drugs are not adsorbed on to the external surface of the nanoparticles. A similar observation has been reported in the literature where nanoparticles characterized using FT-IR did not show the presence of any drug peaks and the drug being investigated was suggested to have been removed during the centrifugation step [12].

### 3.2. Particle size analysis and surface charge

The mean particle size analysis revealed a size range from 190 nm to 480 nm (Table 1) between the different nanoparticle samples. As previously stated, SEM image analysis (Figure 1) of the nanoparticle samples prepared using method 8 showed the majority of the particles to be in the nm size range, which supports the observations made using the zetasizer. Incorporating the drugs into the nanoparticles did not alter the mean particle size significantly compared to the blank PLA nanoparticles. Further, the mean particle size did not vary when the ratio between polymer and drug(s) concentration was altered during the developmental

stage (Table 1). Studies reported in the literature on the formulation of polymeric nanoparticles produced using emulsion methods resulted in nanoparticles in a similar size range to that reported here [12,26,27].

PLA nanoparticles, both blank and drug-loaded prepared using method 8, were measured to have a zeta potential in the range of –13 mV to –19 mV (Table 1). A zeta potential of ±25mV indicate that the samples are stable when present in a suspension [28,29]. A zeta potential of ±20 mV and ±5 mV suggests acceptable stability and short term stability, respectively [30]. The zeta potential for the PLA nanoparticles measured in this study is consistent with the reported literature values, where variation in formulation parameters such as method of synthesis and drug incorporation did not significantly alter the overall negative charge of the nanoparticles [27,31].

### 3.3. Thermal analysis of drug-loaded PLA nanoparticles

The thermal response of the nanoparticle samples was compared to drug and polymer standards in order to determine any similarities and differences as a result of interactions between the components. The thermogram for PLA showed a glass transition peak in the region of 45°C (Figure 3C). A thermogram for the nanoparticles also revealed the presence of a peak at 45°C representing the glass transition of PLA (Figure 3D). These observations indicate that the glass transition phase of the polymer was not influenced by the preparation procedure. The results are similar to a previous study on PLA/PLGA-docetaxel nanoparticles reported by Musumeci et al., [29]. Theophylline and budesonide standards gave sharp, single endothermic peaks at 273°C (Figure 3A) and 261°C (Figure 3B) for theophylline and budesonide, respectively. However, there was an absence of drug peaks for drug-loaded

nanoparticles (Figure 3D). The ratio of polymer to the drug or a possible interaction between the two components may result in the absence of the drug peaks. Alternatively, it has been suggested that a lack of drug peaks in a DSC thermogram can indicate the presence of the encapsulated drug in an amorphous state [27,29,30].

### 3.4. Determination of drug loading efficiency in the PLA nanoparticles

As reviewed by Vrignaud et al. [3232] expressing the drug-loading efficiency based on the amount of drug entrapped in the nanoparticles compared to the amount used in the formulation of the nanoparticles was suggested to be more representative than calculating encapsulation efficiency. Overall a greater loading efficiency was obtained for the hydrophobic drug (budesonide) than the hydrophilic drug (theophylline) in all the nine methods investigated in this study (Table 1). A similar extraction method to the one followed in this study was reported in the literature, where a specific amount of freeze dried nanoparticles were placed in an organic solvent and analyzed to determine the loading efficiency of drugs incorporated into other biodegradable polymeric nanoparticles [12,27]. The highest drug loading reported for a monoencapsulated hydrophilic drug was 20.7% using the DESD method [27] which is similar to the loading efficiency of theophylline in the current study (Table 1).

The drug-loading efficiency of mono-encapsulated nanoparticles of theophylline and budesonide was compared to that of the co-encapsulated nanoparticles. Similar loading efficiency was obtained for both theophylline and budesonide in the mono- and co-encapsulated nanoparticles (Table 1). A higher loading efficiency was obtained for budesonide ($p < 0.05$). Due to its high aqueous solubility, the hydrophilic

drug partitions to the aqueous phase during the nanoparticle preparation resulting in a lower loading efficiency. It has also been previously suggested that the lower loading efficiency of hydrophilic drugs is not only because of diffusion of the drug into the aqueous phase but also because of poor interaction between the drug and the polymer. This poor interaction causes an increased diffusion of the drug from the organic phase to the aqueous phase during the production of the nanoparticles [33,34,35]. However, using a mixed organic phase allows for increased miscibility of the organic phase with the aqueous phase thereby enabling more of the hydrophilic drug to be encapsulated [26].

### 3.5. Drug release from nanoparticles

The aim of formulating theophylline and budesonide nanoparticles using PLA was to obtain a sustained release product. Franz diffusion cells were used to compare the rate of drug release from the nanoparticles with the diffusion rate of the drugs from solutions of theophylline and budesonide at equivalent concentrations to that present in the nanoparticles. Neither drug was bound to the cellulose (dialysis) membrane, which was therefore deemed to be suitable for use. The small pore size (24 Å or 2.4 nm) ensured that only the drug crossed the membrane and prevented nanoparticles entering the receiver chamber. A mixture of SLF and methanol (1:1 v/v) was used in the receiver chamber; it should be recognized that the inclusion of methanol represents a shift from the biological system but permitted an accurate determination of the concentration of both drugs released and ensured solubility was not compromised. The biological system was represented by using the cell culture medium only when studying the permeability of cells to the compounds. At the end of 24 h, 10 – 15% of theophylline was released from both mono- and co-encapsulated

nanoparticles, while for budesonide the drug release from mono- and co-encapsulated nanoparticles was between 3 – 7% at the end of 24 h. There was no significant difference in the percentage of drug released from the mono- and co-encapsulated nanoparticles for both drugs ($p$>0.05) (Figure 4). The percentage of each drug diffusing into the receiver chamber from the solutions was significantly higher than the percentage released from the nanoparticles ($p$<0.05, student's t-test). The rate of drug release at room temperature was not significantly different to the rate of drug release at 37°C, an observation that was also previously reported by Kim and Martin [36]. The release profiles of theophylline and budesonide from the nanoparticles were compared to various mathematical models and the greatest correlation ($r^2$ > 0.9) was observed for the Higuchi model. The Higuchi model has been reported as the model representing the release of drugs from different nanoparticle formulations in previous studies [27,37]. In general, maintenance of sink conditions is essential for determining the release profile or dissolution from a formulation. However, there is a risk of violating sink conditions when using miniaturized techniques, where aggregation of the sample due to limited agitation is also a possibility [38,39]. The presence of a membrane, constant stirring in the Franz diffusion cell and receiver cell concentrations less than 12 µg/ml (10% of initial dose) indicate that sink conditions were maintained in the current study.

### 3.6. Effect of nanoparticles on the viability of 16HBE14o- cells

The concentration range of solutions of theophylline chosen for the assessment of its cytotoxicity included the concentrations likely to be achieved with maximal theoretical loading efficiency of theophylline in the nanoparticles. For instance, a concentration of 5 mg/ml nanoparticles (the maximum used in this study) would be

expected to contain approximately 980 µg/ml theophylline and 98 µg/ml budesonide. This allowed a comparison to be made between the effects of the drugs in solution/suspension and their effects when encapsulated in nanoparticles. The range also included the concentration of nanoparticles used in the drug release studies (0.6 mg/ml). The viability of cells treated with solutions of theophylline and suspensions of budesonide in cell culture medium I at concentrations equivalent to those present in the nanoparticles was similar to the viability of cells treated with co-encapsulated nanoparticles. Theophylline solutions did not affect the viability of cells until the concentration reached 1 mg/ml which decreased the percentage viability of the cells to approximately 75% ($p<0.05$) (Figure 5A). This concentration of theophylline is similar (based on loading efficiency) to that expected to be present in 5 mg/ml mono- and co-encapsulated nanoparticles which also decreased cell viability to average values of approximately 50% and 66%, respectively (Figure 6) ($p<0.05$).

Suspensions of budesonide were not toxic to the cells over the concentration range studied (Figure 5B) although it should be recognized that the aqueous solubility of budesonide is 47.5 µg/ml [3940,41,42]. The toxicity of budesonide to the lung cell lines, Calu-1 and A549 over the concentration range 0.1 – 100 µM (4 ng/ml – 40 µg/ml) was studied by Bandi and Kompella [43]. No toxicity was observed to the Calu-1 cells over this concentration range although the viability of A549 cells was decreased to 43% of the control values at the highest concentration.

Mono- and co-encapsulated nanoparticles containing budesonide did not affect cell viability below a concentration of 5 mg/ml ($p>0.05$) (Figure 6). The inhaled dose of budesonide used clinically is 100 – 200 µg, suggesting that 5 mg/ml is an appropriate upper limit for the study. However, *in vivo* this dose would be available to the entire lung whereas in the current study the nanoparticle suspension (100 µl) is

applied to an area of cells of approximately 0.55 $cm^2$. This would be expected to cause a higher toxicity than would be seen *in vivo* and justifies the exploration of lower concentrations.

### 3.7. Permeability of 16HBE14o- cells to theophylline and budesonide in solution and in nanoparticles

The TER of the 16HBE14o- cell layers measured before each transport experiment was 210.50 ± 30.02 $Ohm.cm^2$ indicating that cells had formed a functional barrier. The effect of solutions of theophylline, budesonide, the mono- and co-encapsulated drugs and blank nanoparticles on the integrity of the barrier was assessed by studying the permeability of the 16HBE14o- cells to FD4, a marker of paracellular diffusion. The Papp of FD4 across control cells ranged from 0.12 ± 0.01 x $10^6$ (n=3) to 0.18 ± 0.01 x $10^6$ (n=9) cm/s over 24 h. This was unaffected by the presence of blank nanoparticles ($p>0.05$) (Table 2). Similarly, the Papp of FD4 across cells treated with solutions of theophylline and budesonide and drug encapsulated nanoparticles was similar to the Papp of FD4 across the control cells for those studies ($p > 0.05$) (Table 2). These results support the findings of the cytotoxicity study suggesting that the nanoparticle formulations are not toxic to the cells.

Similar to the Franz diffusion cell studies, the permeability of the cells to theophylline and budesonide released from nanoparticles was compared to the permeability of the cells to the drugs when applied to the cells in solution. The results indicated that the drugs applied as nanoparticles crossed the cells more slowly than when presented as a solution and that the nanoparticles were able to provide sustained release.

After 6 h, 3.69% of the theophylline co-encapsulated in the nanoparticles was transported across the cells in comparison to 8.25% of theophylline from a solution of equivalent concentration (Figure 7A). The average Papp for the theophylline solution over the time period 6-24 h shows a reduction in comparison to that over 0-6 h ($p<0.05$) (Table 3). This was not paralleled by the Papp of the co-delivered FD4 solution where the diffusion rate was approximately linear over the entire 24 h experiment and may indicate that sink conditions for theophylline were approached/exceeded. Over 24 h, the Papp of the theophylline applied as a solution was $1.29 \pm 0.23 \times 10^{-6}$ cm/s, compared to Papp values of $0.61 \pm 0.33$ and $0.81 \pm 0.23 \times 10^{-6}$ cm/s for theophylline released from the mono- and co-encapsulated nanoparticles, respectively. It is likely that the water-soluble theophylline is released fairly readily from the nanoparticles into the aqueous environment of the cell culture medium; the mechanism of drug release from the nanoparticles could be a quick burst release followed by a slow release. It is likely that the transport of theophylline across the cells is *via* paracellular diffusion similar to FD4 as a result of the similar log P values of the two compounds.

The transport of budesonide across the 16HBE14o- cells was also more rapid when applied in solution than when applied as nanoparticles, consistent with the results obtained for theophylline. However, at 6 h, budesonide showed less than 1% of the initial concentration transported across the cell monolayer from the budesonide solutions (Figure 7B). The average Papp for the budesonide solution over the time period 6-24 h shows a reduction in comparison to that over 0-6 h ($p<0.05$) (Table 3), again not paralleled by the co-delivered FD4. Over 24 h, the Papp of the budesonide applied as a solution was $0.12 \pm 0.05 \times 10^{-6}$ cm/s, compared to Papp values of $0.02 \pm 0.01$ and $0.05 \pm 0.00 \times 10^{-6}$ cm/s for budesonide released

from the mono- and co-encapsulated nanoparticles, respectively (Table 3). The slower transport rate of budesonide across the cells from the mono- and co-encapsulated nanoparticles is thought to be due to transport of budesonide being dependent on release of the drug from the nanoparticles (rate-limiting step). By being present in an unfavorable aqueous environment, the release of budesonide from mono- and co-encapsulated nanoparticles may be further reduced and was less than 1% after a period of 24 h. Further work would be required to confirm these observations.

Generally, more lipophilic compounds e.g. budesonide would be expected to diffuse across the cells faster than hydrophilic compounds of similar molecular weight e.g. theophylline [44]. In this study that is not the case and may be explained by uptake and retention of budesonide within the cells as a result of intracellular esterification and conjugation to fatty acids [45,46,47,48].

### 3.8. Deposition of nebulized drug-loaded nanoparticles using the MSLI

A major proportion of nanoparticles (and therefore drugs) remained in the chamber of the nebulizer when the suspension was nebulized. This amounted to 41.21 ± 7.95% for theophylline and 27.48 ± 11.60% for budesonide; whether they were delivered as co- or mono-encapsulated nanoparticle suspension (Figure 8). A high percentage of theophylline was recovered from stages 3-5 (nebulized droplet size <6.8 µm). Interestingly, when the co-encapsulated drugs were nebulized 75.02 ± 20.69% of theophylline was calculated in the FPF (where particle size is <6.8 µm) while this was only 48.90 ± 14.94% for budesonide. The FPF for mono-encapsulated nanoparticles was calculated to be 69.26 ± 19.23% for theophylline and 20.31 ± 4.18% for budesonide. The Mass Median Aerodynamic Diameter (MMAD) for

droplets consisting of theophylline and budesonide from co-encapsulated nanoparticles was calculated to be 2.63 µm and 2.30 µm, respectively. For mono-encapsulated nanoparticles, the droplet MMAD was calculated to be 2.30 µm and 3.54 µm for the formulation containing the theophylline and budesonide, respectively. The results indicate that with the droplet size being < 5 µm and a relatively high FPF for theophylline and budesonide in the co-encapsulated nanoparticles, the formulation is suitable for inhalation. Despite the variation in drug loading the observations made from the deposition study indicate that these drugs could be administered to the appropriate area of the lung, depending on the type of drug delivery device.

## 4. Conclusions

In summary, budesonide and theophylline were successfully co-encapsulated in PLA nanoparticles using a modified DESD method. The procedure variables were optimized to encapsulate both the hydrophobic and hydrophilic drugs and could potentially be further adapted to incorporate other drugs with differing aqueous solubility. The nanoparticles characterized in this study possessed a narrow size distribution and zeta potential with good drug-loading efficiency for both hydrophilic and hydrophobic drugs, making them suitable to be developed into a formulation for pulmonary drug delivery. Drug release from the nanoparticles over a period of 24 h showed their capability for sustained drug release. Similar release profiles were obtained for both budesonide and theophylline from both mono- and co-encapsulated nanoparticles. In a clinical situation this would avoid the need for multiple inhalers and also allow the dosing interval to be increased which can be expected to increase patient compliance. Sustained release could also reduce the occurrence of adverse effects. Cytotoxicity and permeability studies showed the nanoparticle formulations to be well-tolerated by airway cells at clinically relevant concentrations. Further, permeability studies supported the sustained release of the drugs from the nanoparticles observed in earlier studies. Nebulization of nanoparticle suspensions showed successful drug deposition in stages 3 to 5 (particle size <6.8 μm) with a good overall recovery of the nanoparticles. This indicates that, despite their small size, the nanoparticles are able to target the appropriate area of the lung when delivered using a nebulizer. Thus, these nanoparticles are suitable to provide a new therapeutic strategy for pulmonary drug delivery.

## Author contributions

Planning of the research work was equally shared between MDB, ABL, SS and ASP. Research work was carried out by MDB. All authors have contributed equally in the preparation of the manuscript and have given their consent to the final version of the manuscript.

## Declaration of interest

Authors declare that there is no conflict of interest.


## Acknowledgements

MDB would like to thank the University of Brighton for the PhD scholarship award. This research did not receive any specific grant from funding agencies in the public, commercial or not-for-profit organizations.

## References


1. Mancarella, S., Greco, V., Baldassarre, F., Vergara, D., Maffia, M., Leporatti, S., 2015. Polymer-Coated Magnetic Nanoparticles for Curcumin Delivery to Cancer Cells. Macromol Biosci. 15, 1365-1374. https://doi.org/10.1002/mabi.201500142

2. Wang, B., Tang, Y., Oh, Y., Lamb, N.W., Xia, S., Ding, Z., Chen, B., Suárez, M.J., Meng, T., Kulkarni, V., Eberhart, C.G., Ensign, L.M., Stark, W.J., Hanes, J., Xu, Q., 2019. Controlled release of dexamethasone sodium phosphate with biodegradable nanoparticles for preventing experimental corneal neovascularization. Nanomed. Jan 21. pii: S1549-9634(19)30012-7. https://doi.org/10.1016/j.nano.2019.01.001

3. Vergara, D., Bellomo, C., Zhang, X., Vergaro, V., Tinelli, A., Lorusso, V., Rinaldi, R., Lvov, Y.M., Leporatti, S., Maffia, M., 2012. Lapatinib/Paclitaxel polyelectrolyte nanocapsules for overcoming multidrug resistance in ovarian cancer. Nanomed. 8, 891-899. https://doi.org/10.1016/j.nano.2011.10.014

4. Reis, C.P., Neufeld, R.J., Ribeiro, A.J., Veiga, F., 2006. Nanoencapsulation I. Methods for preparation of drug-loaded polymeric nanoparticles. Nanomed-Nanotechnol. 2, 8-21. https://doi.org/10.1016/j.nano.2005.12.003

5. Sinha, V.R., Bansal, K., Kaushik, R., Kumria, R., Trehan, A., 2004. Poly-epsilon-caprolactone microspheres and nanospheres: an overview. Int. J. Pharm. 278, 1-23. https://doi.org/10.1016/j.ijpharm.2004.01.044

6. Kumari, A., Yadav, S.K., Yadav, S.C., 2010. Biodegradable polymeric nanoparticles based drug delivery systems. Colloids Surf. B Biointerfaces. 75, 1-18. https://doi.org/10.1016/j.colsurfb.2009.09.001

7. Merkeli, A, Tabatabay, C., Gurny, R., Heller, J., 1998. Biodegradable polymers for the controlled release of ocular drugs. Prog. Polym. Sci. 23, 563-580. https://doi.org/10.1016/S0079-6700(97)00048-8

8. Gasparini, G., Holdich, R.G., Kosvintsev, S.R., 2010. PLGA particle production for water-soluble drug encapsulation: degradation and release behaviour. Colloids Surf. B Biointerfaces. 75, 557-564. https://doi.org/10.1016/j.colsurfb.2009.09.035

9. Panyam, J., Labhasetwar, V., 2012. Biodegradable nanoparticles for drug and gene delivery to cells and tissue. Adv. Drug Deliv. Rev. 64, 61-71. https://doi.org/10.1016/S0169-409X(02)00228-4

10. Nolan, L.M., Tajber, L., McDonald, B.F., Barham, A.S., Corrigan, O.I., Healy, A.M., 2009. Excipient-free nanoporous microparticles of budesonide for pulmonary delivery. Eur. J. Pharm. Sci. 37, 593-602. https://doi.org/10.1016/j.ejps.2009.05.007

11. El-Gendy, N., Pornputtapitak, W., Berkland, C., 2011. Nanoparticle agglomerates of fluticasone propionate in combination with albuterol sulfate as dry powder aerosols. Eur. J. Pharm. Sci. 44, 522-533. https://doi.org/10.1016/j.ejps.2011.09.014

12. Sinha, B., Mukherjee, B., Pattnaik, G., 2013. Poly-lactide-co-glycolide nanoparticles containing voriconazole for pulmonary delivery: in vitro and in vivo study. Nanomedicine. 9, 94-104. https://doi.org/10.1016/j.nano.2012.04.005

13. Merchant, Z., Taylor, K.M.G., Stapleton, P., Razak, S.A., Kunda, N., Alfagih, I., Sheikh, K., Saleem, I.Y., Somavarapu, S., 2014. Engineering hydrophobically modified chitosan for enhancing the dispersion of respirable

microparticles of levofloxacin. Eur. J. Pharm. Biopharm. 88, 816-829. https://doi.org/10.1016/j.ejpb.2014.09.005

14. Sharma, K., Somavarapu, S., Colombani, A., Govind, N., Taylor, K.M.G., 2013. Nebulised siRNA encapsulated crosslinked chitosan nanoparticles for pulmonary drug delivery. Int. J. Pharm. 455, 241-247. https://doi.org/10.1016/j.ijpharm.2013.07.024

15. Ungaro, F., d'Angelo, I., Coletta, C., d'Emmanuele di Villa Bianca, R., Sorrentino, R., Perfetto, B., Tufano, M.A., Miro, A., La Rotonda, M.I., Quaglia, F., 2012. Dry powders based on PLGA nanoparticles for pulmonary delivery of antibiotics: modulation of encapsulation efficiency, release rate and lung deposition pattern by hydrophilic polymers. J. Control. Release. 157, 149-159. https://doi.org/10.1016/j.jconrel.2011.08.010

16. Roa, W.H., Azarmi, S., Al-Hallak, M.H., Finlay, W.H., Magliocco, A.M., Lobenberg, R., 2011. Inhalable nanoparticles, a non-invasive approach to treat lung cancer in a mouse model. J. Control. Release. 150, 49-55. https://doi.org/10.1016/j.jconrel.2010.10.035

17. Klingler, C., Müller, B.W., Steckel, H., 2009. Insulin-micro- and nanoparticles for pulmonary delivery. Int. J. Pharm. 377, 173-179. https://doi.org/10.1016/j.ijpharm.2009.05.008

18. Yeh, H-W., Chen, D-R., 2017. *In vitro* release profiles of PLGA core-shell composite particles loaded with theophylline and budesonide. Int. J. Pharm. 528, 637-645. https://doi.org/10.1016/j.ijpharm.2017.06.032

19. Al Malyan, M., Becchi, C., Nikkola, L., Viitanen, P., Boncinelli, S., Chiellini, F., Ashammakhi, N., 2006. Polymer-based biodegradable drug delivery

systems in pain management. J. Craniofac. Surg. 17, 302-313. https://doi.org/10.1097/00001665-200603000-00018

20. Tran, S., DeGiovanni, P-J., Piel, B., Rai, P., 2017. Cancer nanomedicine: a review of recent success in drug delivery. Clin. Trans. Med. 6:44, 1-21. https://doi.org/10.1186/s40169-017-0175-0

21. Locatelli, E., Franchini, M.C., 2012. Biodegradable PLGA-b-PEG polymeric nanoparticles: synthesis, properties, and nanomedical application as drug delivery system. J. Nanopart. Res. 14:1316. https://doi.org/10.1007/s11051-012-1316-4

22. Li, Z., Liu, K., Sun, P., Mei, L., Hao, T., Tian, Y., Tang, Z., Li, L., Chen, D., 2013. Poly(D, L-lactide-co-glycolide)/montmorillonite nanoparticles for improved oral delivery of exemestane. J. Microencap. 30, 432-440. https://doi.org/10.3109/02652048.2012.746749

23. Marques, M.R.C., Loebenberg, R., Almukainzi, M., 2011. Simulated biological fluids with possible application in dissolution testing. Dissolut. Technol. 18, 15-28. https://dx.doi.org/10.14227/DT180311P15

24. Lai, P., Daear, W., Lobenberg, R., Prenner, E.J., 2014. Overview of the preparation of organic polymeric nanoparticles for drug delivery based on gelatine, chitosan, poly(d.l-lactide-co-glycolic acid) and polyalkylcyanoacrylate. Colloids Surf. B. Bioterfaces. 118, 154-163. https://doi.org/10.1016/j.colsurfb.2014.03.017

25. Zambaux, M.F., Bonneaux, F., Gref, R., Maincent, P., Dellacherie, E., Alonso, M.J., Labrude, P., Vigneron, C., 1998. Influence of experimental parameters on the characteristics of poly(lactic acid) nanoparticles prepared

by a double emulsion method. J. Control. Release. 50(1–3), 31-40. https://doi.org/10.1016/S0168-3659(97)00106-5

26. Cheow, W.S., Hadinoto, K., 2010. Enhancing encapsulation efficiency of highly water-soluble antibiotic in poly(lactic-co-glycolic acid) nanoparticles: Modifications of standard nanoparticle preparation methods. Colloids and Surfaces A: Physicochem. Eng. Aspects. 370, 79–86. https://doi.org/10.1016/j.colsurfa.2010.08.050

27. Miladi, K., Sfar, S., Fessi, H., Elaissari, A., 2015. Encapsulation of alendronate sodium by nanoprecipitation and double emulsion: From preparation to in vitro studies. Ind. Crop. Prod. 72, 24-33. https://doi.org/10.1016/j.indcrop.2015.01.079

28. Singh, R., Lillard, J.W.Jr., 2009. Nanoparticle-based targeted drug delivery. Exp. Mol. Pathol. 86, 215-223. https://doi.org/10.1016/j.yexmp.2008.12.004

29. Musumeci, T., Ventura, C.A., Giannone, I., Ruozi, B., Montenegro, L., Pignatello, R., Puglisi, G., 2006. PLA/PLGA nanoparticles for sustained release of docetaxel. Int. J. Pharm. 325, 172-179. https://doi.org/10.1016/j.ijpharm.2006.06.023

30. Wu, L., Zhang, J., Watanabe, W., 2011. Physical and chemical stability of drug nanoparticles. Adv. Drug Deliv. Rev. 63, 456-469. https://doi.org/10.1016/j.addr.2011.02.001

31. Tiwari, M.N., Agarwal, S., Bhatnagar, P., Singhal, N.K., Tiwari, S.K., Kumar, P., Chauhan, L.K., Patel, D.K., Chaturvedi, R.K., Singh, M.P., Gupta, K.C., 2013. Nicotine-encapsulated poly(lactic-co-glycolic) acid nanoparticles improve neuroprotective efficacy against MPTP-induced parkinsonism. Free

Radic. Biol. Med. 65, 704-718. https://doi.org/10.1016/j.freeradbiomed.2013.07.042

32. Vrignaud, S., Benoit, J.P., Saulnier, P., 2011. Strategies for the nanoencapsulation of hydrophilic molecules in polymer-based nanoparticles. Biomaterials. 32, 8593-8604. https://doi.org/10.1016/j.biomaterials.2011.07.057

33. Budhian, A., Siegel, S.J., Winey, K.I., 2007. Haloperidol-loaded PLGA nanoparticles: systematic study of particle size and drug content. Int. J. Pharm. 336, 367-375. https://doi.org/10.1016/j.ijpharm.2006.11.061

34. Manchanda, R., Fernandez-Fernandez, A., Nagesetti, A., McGoron, A.J., 2010. Preparation and characterization of a polymeric (PLGA) nanoparticulate drug delivery system with simultaneous incorporation of chemotherapeutic and thermo-optical agents. Colloids Surf. B Biointerfaces. 75, 260-267. https://doi.org/10.1016/j.colsurfb.2009.08.043

35. Barichello, J.M., Morishita, M., Takayama, K., Nagai, T., 1999. Encapsulation of hydrophilic and lipophilic drugs in PLGA nanoparticles by the nanoprecipitation method. Drug Dev. Ind. Pharm. 25, 471-476. https://doi.org/10.1081/DDC-100102197

36. Kim, D.H., Martin, D.C., 2006. Sustained release of dexamethasone from hydrophilic matrices using PLGA nanoparticles for neural drug delivery. Biomaterials. 27, 3031-3037. https://doi.org/10.1016/j.biomaterials.2005.12.021

37. Gandhi, A., Jana, S., Sen, K.K., 2014. In-vitro release of acyclovir loaded Eudragit RLPO(®) nanoparticles for sustained drug delivery. Int. J. Biol. Macromol. 67, 478-482. https://doi.org/10.1016/j.ijbiomac.2014.04.019

38. Zolnik, B.S., Raton, J-L., Burgess, D.J., 2005. Application of USP apparatus 4 and in situ fiber optic analysis to microsphere release testing. Dissol. Technol. 12, 11-14. https://dx.doi.org/10.14227/DT120205P11

39. Wischke, C., Schwendeman, S.P., 2008. Principles of encapsulating hydrophobic drugs in PLA/PLGA microparticles. Int. J. Pharm. 364, 298-327. https://doi.org/10.1016/j.ijpharm.2008.04.042

40. Szefler, S.J., 1999. Pharmacodynamics and pharmacokinetics of budesonide: a new nebulized corticosteroid. J. Allergy Clin. Immunol. 104, 175-183. https://doi.org/10.1016/S0091-6749(99)70059-X

41. Szefler, S.J. Eigen, H., 2002. Budesonide inhalation suspension: a nebulized corticosteroid for persistent asthma. J. Allergy Clin. Immunol. 109, 730- 742. https://doi.org/10.1067/mai.2002.122712

42. Bhatt, H., Naik, B., Dharamsi, A., 2014. Solubility Enhancement of Budesonide and Statistical Optimization of Coating Variables for Targeted Drug Delivery. J. Pharm. 2014, 262194, 1-13. http://dx.doi.org/10.1155/2014/262194

43. Bandi, N., Kompella, U.B., 2001. Budesonide reducesvascular endothelial growth factor secretion and expression in Calu-1 and alveolar A549 epithelial cells. Eur. J. Pharmacol. 425, 109-116. https://doi.org/10.1016/S0014-2999(01)01192-X

44. Forbes, B., Shah, A., Martin, G.P., Lansley, A.B., 2003. The human bronchial epithelial cell line 16HBE14o− as a model system of the airways for studying drug transport. Int. J. Pharm. 257, 161-167. https://doi.org/10.1016/S0378-5173(03)00129-7

45. Lexmüller, K., Gullstrand, H., Axelsson, B.O., Sjölin, P., Korn, S.H., Silberstein, D.S., Miller-Larsson, A., 2007. Differences in endogenous esterification and retention in the rat trachea between budesonide and ciclesonide active metabolite. Drug Metab. Dispos. 35, 1788-1796. https://doi.org/10.1124/dmd.107.015297

46. Wieslander, E., Delander, E.L., Jarkelid, L., Hjertberg, E., Tunek, A., Brattsand, R., 1998. Pharmacologic importance of the reversible fatty acid conjugation of budesonide studied in a rat cell line in vitro. Am. J. Respir. Cell Mol. Biol. 19, 477-484. https://doi.org/10.1165/ajrcmb.19.3.3195

47. Borchard, G., Cassara, M.L., Roemele, P.E., Florea, B.I., Junginger, H.E., 2002. Transport and local metabolism of budesonide and fluticasone propionate in a human bronchial epithelial cell line (Calu-3). J. Pharm. Sci. 91, 1561-1567. https://doi.org/10.1002/jps.10151

48. Miller-Larsson, A., Mattsson, H., Hjertberg, E., Dahlback, M., Tunek, A., Brattsand, R., 1998. Reversible fatty acid conjugation of budesonide. Novel mechanism for prolonged retention of topically applied steroid in airway tissue. Drug Metab. Dispos. 26, 623-630. http://www.ncbi.nlm.nih.gov/pubmed/9660844

**Figure Captions:**

**Figure 1:** SEM image of blank (A), mono-encapsulated budesonide (B), mono-encapsulated theophylline (C) and co-encapsulated theophylline and budesonide (D) nanoparticles prepared using method 8. SEM images show spherical nanoparticles and wide distribution of particle size.

**Figure 2:** FT-IR spectra of (A) PLA standard, (B) budesonide standard, (C) theophylline standard, and (D) theophylline and budesonide co-encapsulated PLA nanoparticles.

**Figure 3:** DSC thermograms for (A) theophylline standard, (B) budesonide standard, (C) PLA standard and a (D) theophylline and budesonide co-encapsulated PLA nanoparticle.

**Figure 4:** Release of theophylline (A) and budesonide (B) from mono- and co-encapsulated nanoparticles compared to the drug release from a solution of equivalent drug concentration. The percentage of the drug in the receiver chamber from the solution was significantly higher than the percentage released from the nanoparticles at all time points (*$P$<0.05). Similar release was obtained for theophylline and budesonide from both the mono-encapsulated and co-encapsulated nanoparticles except at 24 h (n=6, mean ± SD; **$P$<0.05).

**Figure 5:** The effect of theophylline (A) and budesonide (B) on the percentage viability of 16HE14o- cells when the theophylline solutions were prepared in cell culture medium (n=8, mean ± SD; *$P$<0.05, compared to control).

**Figure 6**: The effect of theophylline mono-encapsulated nanoparticles (A), budesonide mono-encapsulated nanoparticles (B) and theophylline and budesonide co-encapsulated nanoparticles (C) on the percentage viability of 16HE14o- cells. (n=32, mean ± SD) (*$P$<0.05, compared to control). 5 mg/ml nanoparticles contain

approximately 980 µg/ml of theophylline and 98 µg/ml of budesonide (calculated based on loading efficiency).

**Figure 7**: The transport of theophylline (A) and budesonide (B) across the 16HBE14o- cells comparing theophylline and budesonide solutions with mono- and co-encapsulated nanoparticles (n=9, mean ± SD) (*$P$<0.05, solutions compared to nanoparticles at 24 h).

**Figure 8:** Comparison of the deposition profiles of theophylline (A) and budesonide (B) from mono- and co-encapsulated nanoparticles in the different stages of the MSLI when delivered as a nebulized suspension. Percentage amount of theophylline and budesonide recovered from each stage of MSLI, throat and device as determined by HPLC, expressed as a percentage of total recovered dose (n=3, mean ± SD) ($P$>0.05 for theophylline mono- and co-encapsulated nanoparticles) (*$P$< 0.05 for budesonide mono- and co-encapsulated nanoparticles, stage 5).

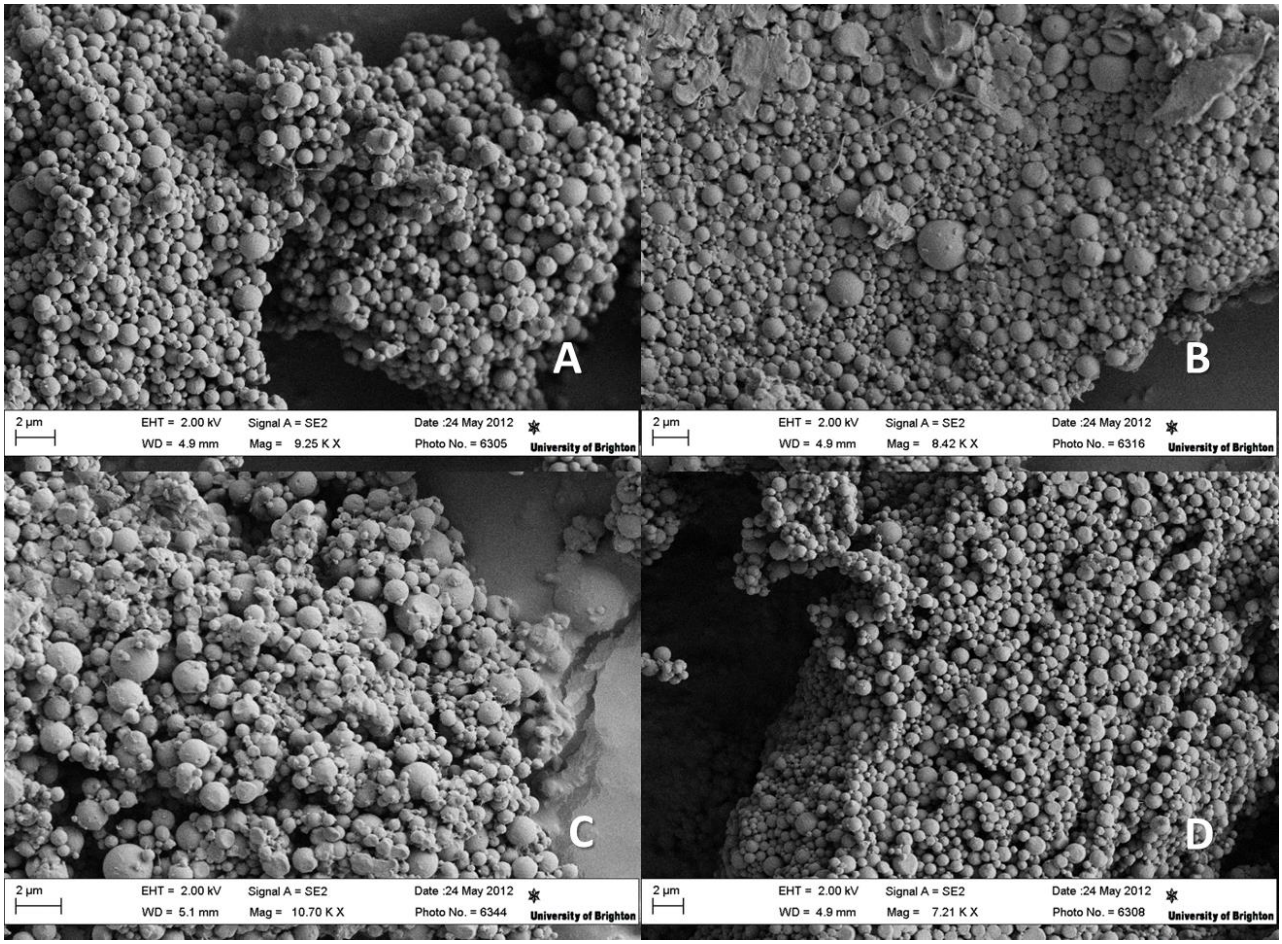
A
2 µm
EHT = 2.00 kV
WD = 4.9 mm
Signal A = SE2
Mag = 9.25 K X
Date :24 May 2012
Photo No. = 6305
University of Brighton
B
2 µm
EHT = 2.00 kV
WD = 4.9 mm
Signal A = SE2
Mag = 8.42 K X
Date :24 May 2012
Photo No. = 6316
University of Brighton
C
2 µm
EHT = 2.00 kV
WD = 5.1 mm
Signal A = SE2
Mag = 10.70 K X
Date :24 May 2012
Photo No. = 6344
University of Brighton
D
2 µm
EHT = 2.00 kV
WD = 4.9 mm
Signal A = SE2
Mag = 7.21 K X
Date :24 May 2012
Photo No. = 6308
University of Brighton

**Figure 1**

905

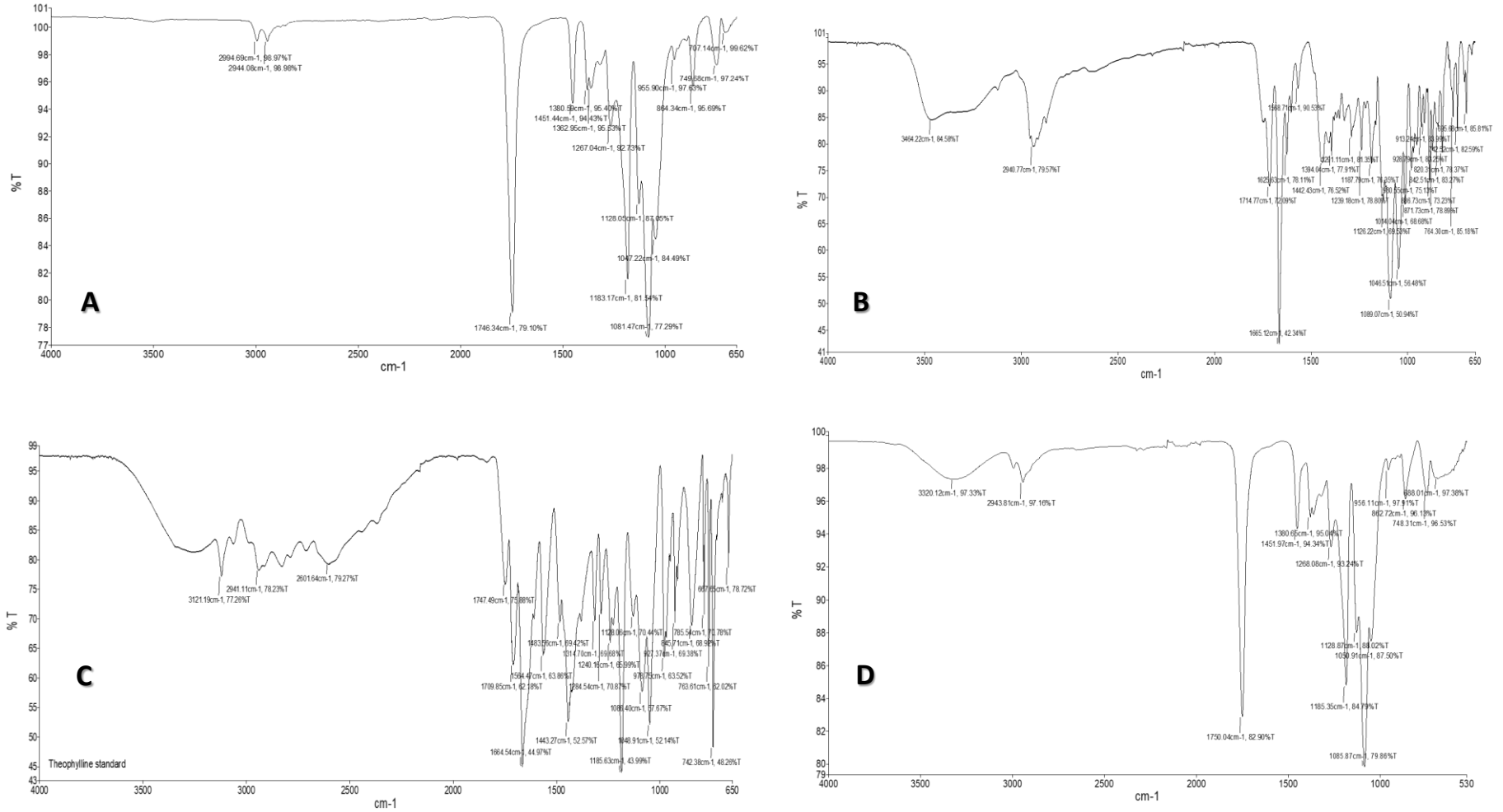
A
% T
cm-1
2994.69cm-1, 98.97%T
2944.08cm-1, 98.98%T
1746.34cm-1, 79.10%T
1380.59cm-1, 95.40%T
1451.44cm-1, 94.43%T
1362.95cm-1, 95.53%T
1267.04cm-1, 92.73%T
955.90cm-1, 97.63%T
884.34cm-1, 95.69%T
797.14cm-1, 99.62%T
749.68cm-1, 97.24%T
1128.05cm-1, 87.95%T
1047.22cm-1, 84.49%T
1183.17cm-1, 81.54%T
1081.47cm-1, 77.29%T
B
% T
cm-1
3464.22cm-1, 84.58%T
2940.77cm-1, 79.57%T
1714.77cm-1, 82.09%T
1685.12cm-1, 42.34%T
1046.51cm-1, 56.48%T
1089.07cm-1, 50.94%T
C
Theophylline standard
% T
cm-1
3121.19cm-1, 77.26%T
2941.11cm-1, 78.23%T
2601.64cm-1, 79.27%T
1747.49cm-1, 75.88%T
1709.85cm-1, 62.18%T
1664.54cm-1, 44.97%T
1443.27cm-1, 52.57%T
1185.63cm-1, 43.99%T
1048.91cm-1, 52.14%T
742.38cm-1, 48.26%T
D
% T
cm-1
3320.12cm-1, 97.33%T
2943.81cm-1, 97.16%T
1750.04cm-1, 82.90%T
1451.97cm-1, 94.34%T
1268.08cm-1, 93.24%T
1128.87cm-1, 88.02%T
1050.91cm-1, 87.50%T
1185.35cm-1, 84.79%T
1085.87cm-1, 79.86%T

**Figure 2**

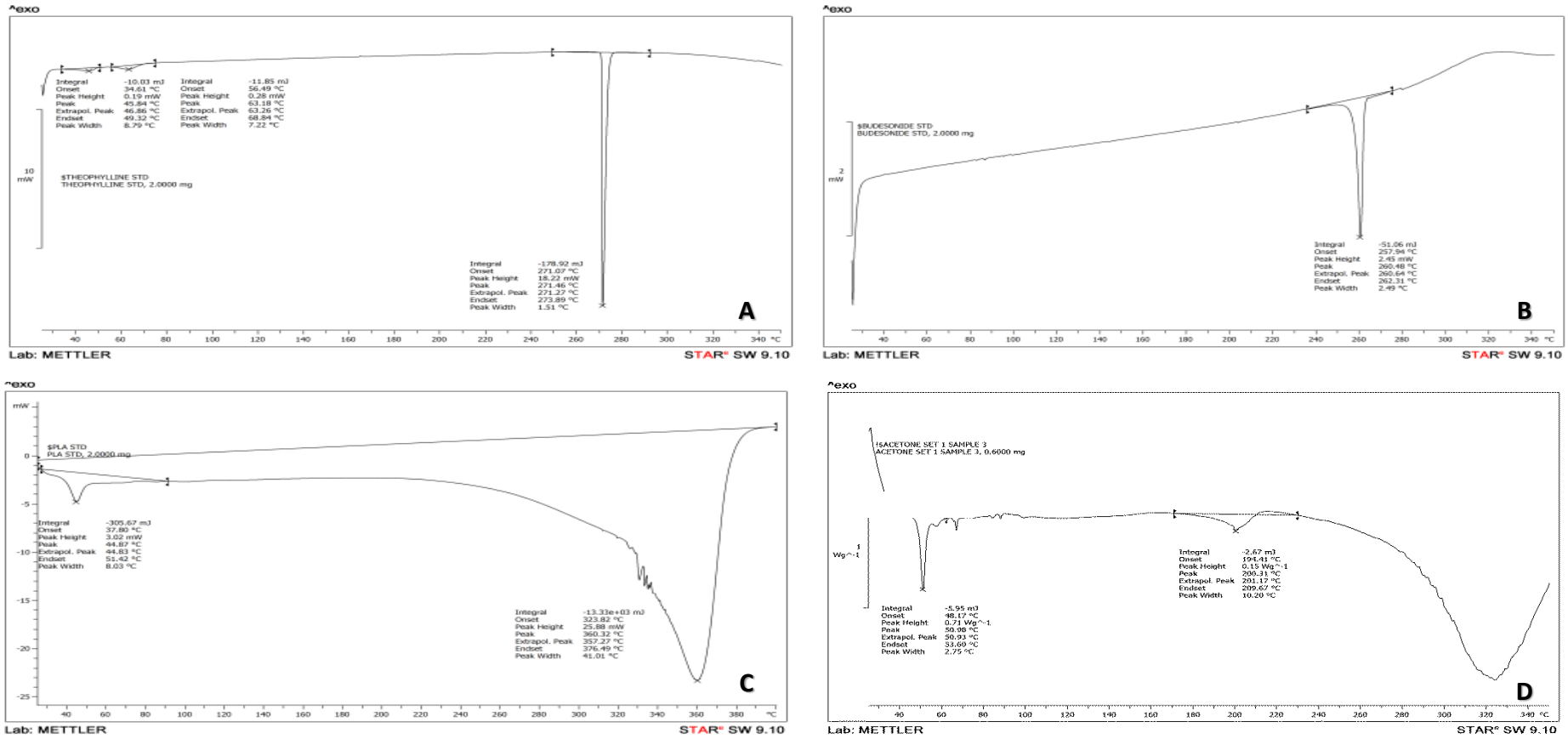
^exo
$THEOPHYLLINE STD
THEOPHYLLINE STD, 2.0000 mg
A
Lab: METTLER
STAR° SW 9.10
$BUDESONIDE STD
BUDESONIDE STD, 2.0000 mg
B
Lab: METTLER
STAR° SW 9.10
$PLA STD
PLA STD, 2.0000 mg
C
Lab: METTLER
STAR° SW 9.10
!ACETONE SET 1 SAMPLE 3
ACETONE SET 1 SAMPLE 3, 0.6000 mg
D
Lab: METTLER
STAR° SW 9.10

910

**Figure 3**

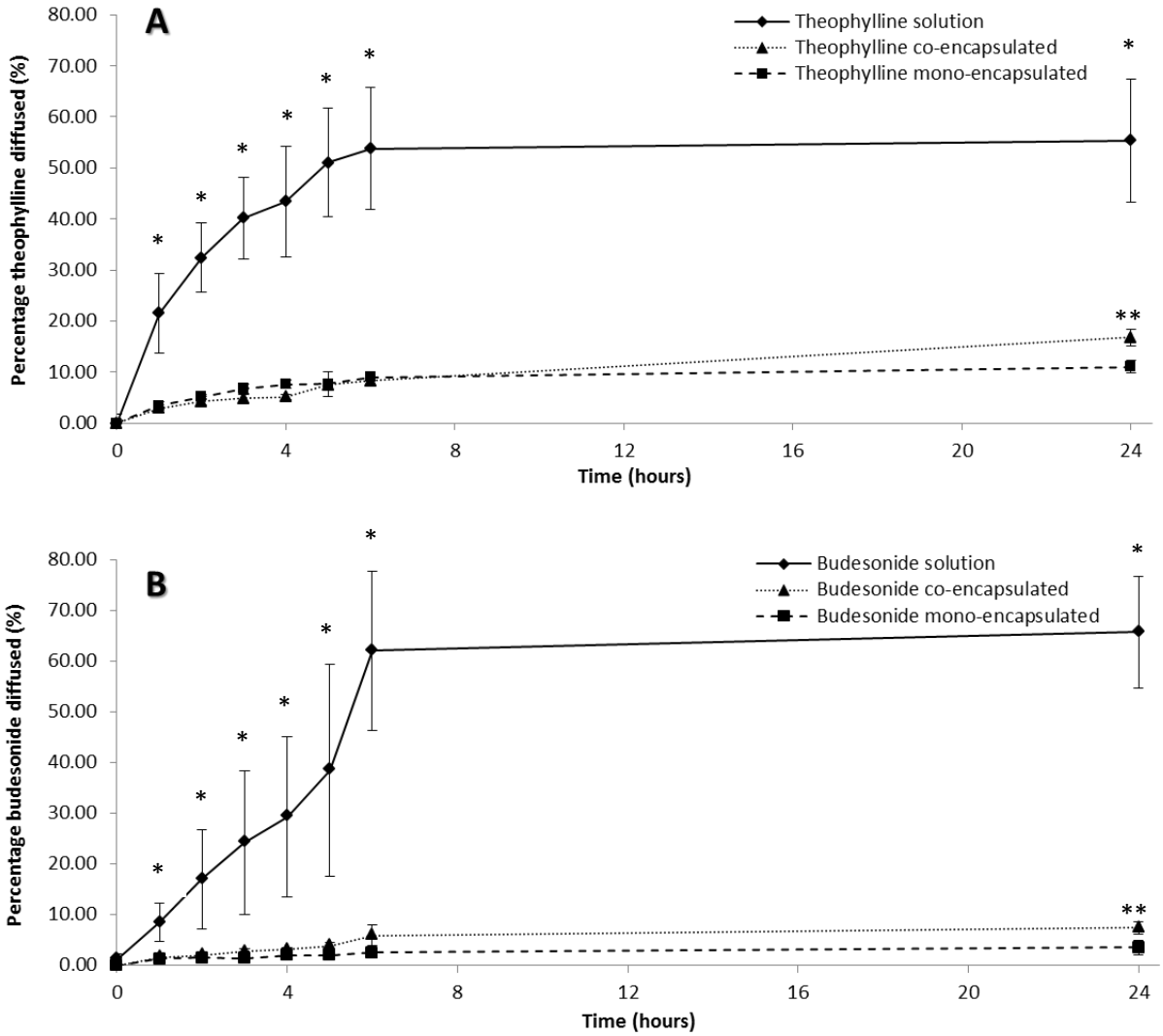
A
Theophylline solution
Theophylline co-encapsulated
Theophylline mono-encapsulated
Percentage theophylline diffused (%)
Time (hours)
B
Budesonide solution
Budesonide co-encapsulated
Budesonide mono-encapsulated
Percentage budesonide diffused (%)
Time (hours)

915

**Figure 4**

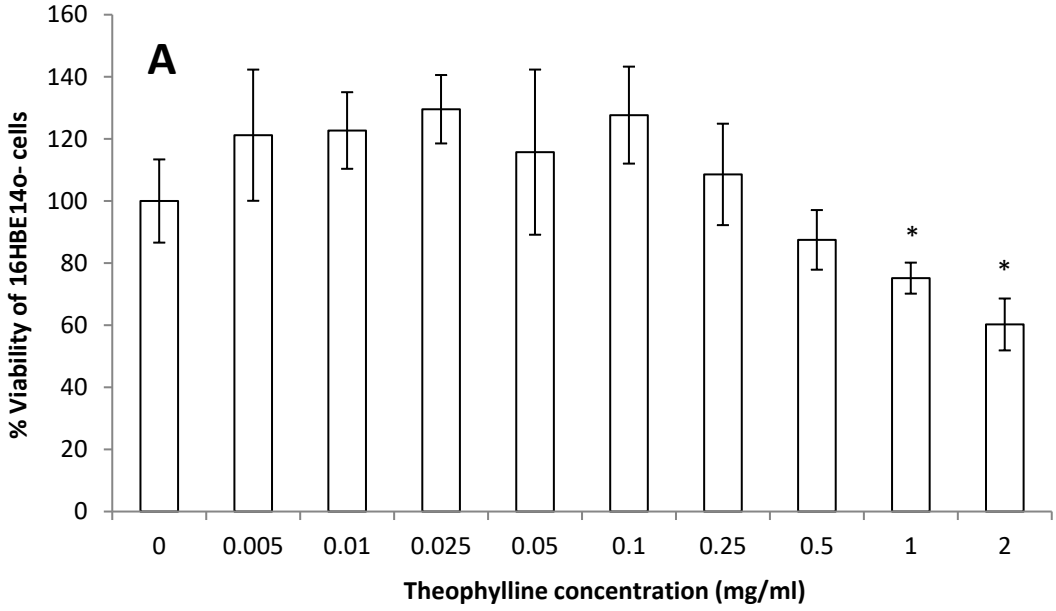
A
% Viability of 16HBE14o- cells
160
140
120
100
80
60
40
20
0
0
0.005
0.01
0.025
0.05
0.1
0.25
0.5
1
2
*
*
Theophylline concentration (mg/ml)

920

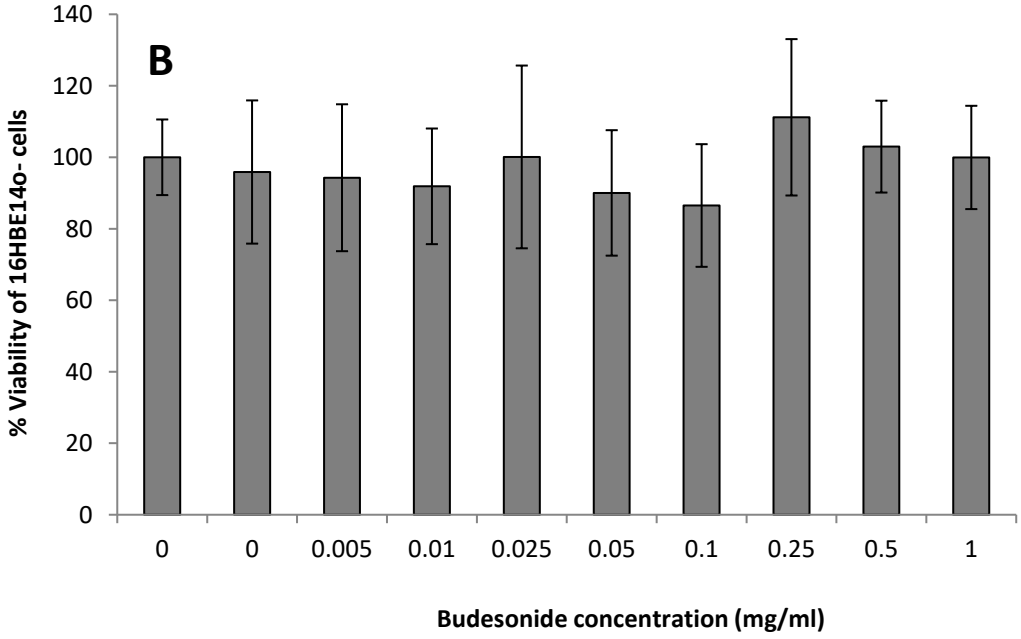
B
% Viability of 16HBE14o- cells
140
120
100
80
60
40
20
0
0
0
0.005
0.01
0.025
0.05
0.1
0.25
0.5
1
Budesonide concentration (mg/ml)

**Figure 5**

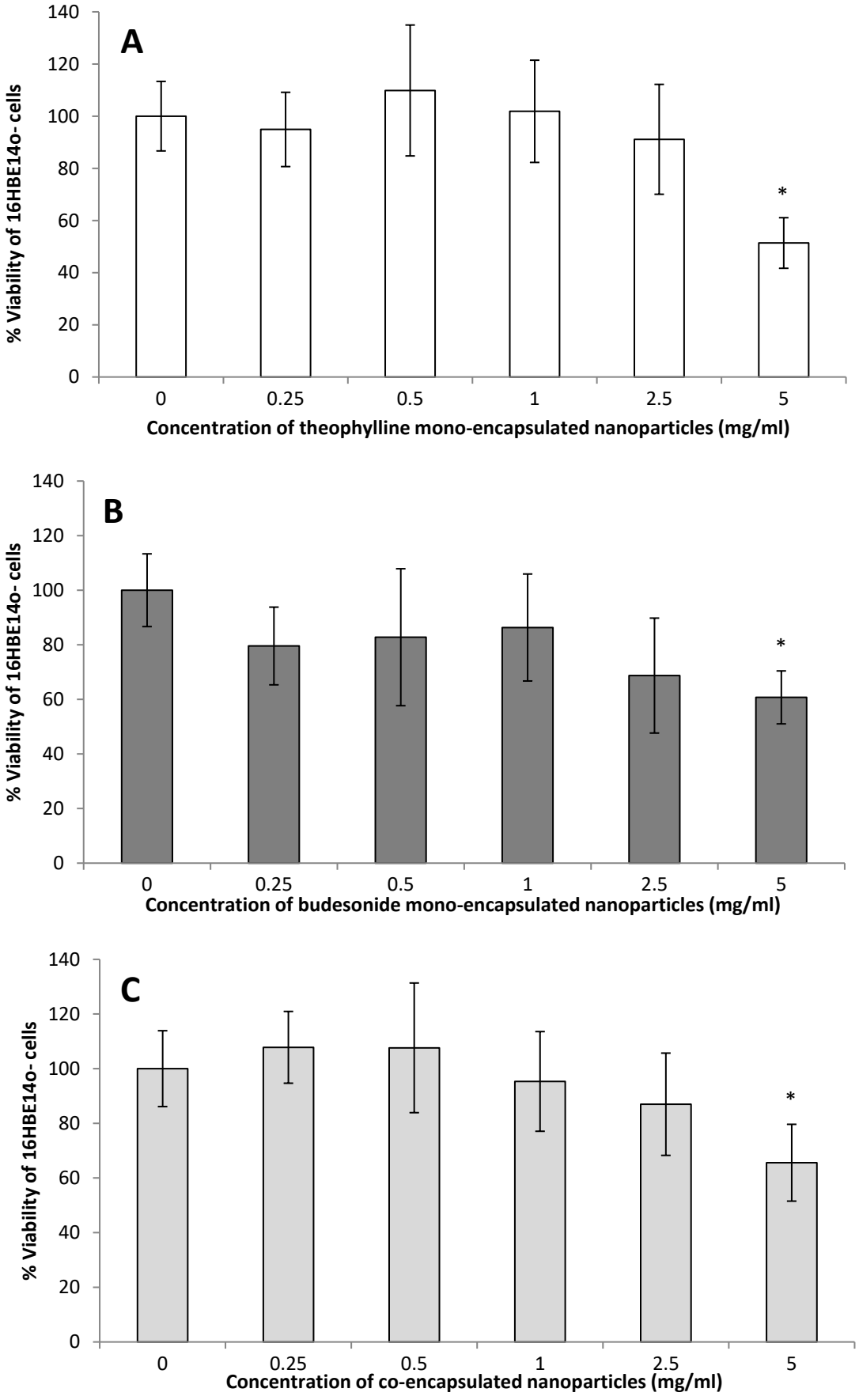
A
% Viability of 16HBE14o- cells
140
120
100
80
60
40
20
0
0
0.25
0.5
1
2.5
5
*
Concentration of theophylline mono-encapsulated nanoparticles (mg/ml)
B
% Viability of 16HBE14o- cells
Concentration of budesonide mono-encapsulated nanoparticles (mg/ml)
C
% Viability of 16HBE14o- cells
Concentration of co-encapsulated nanoparticles (mg/ml)

925

**Figure 6**

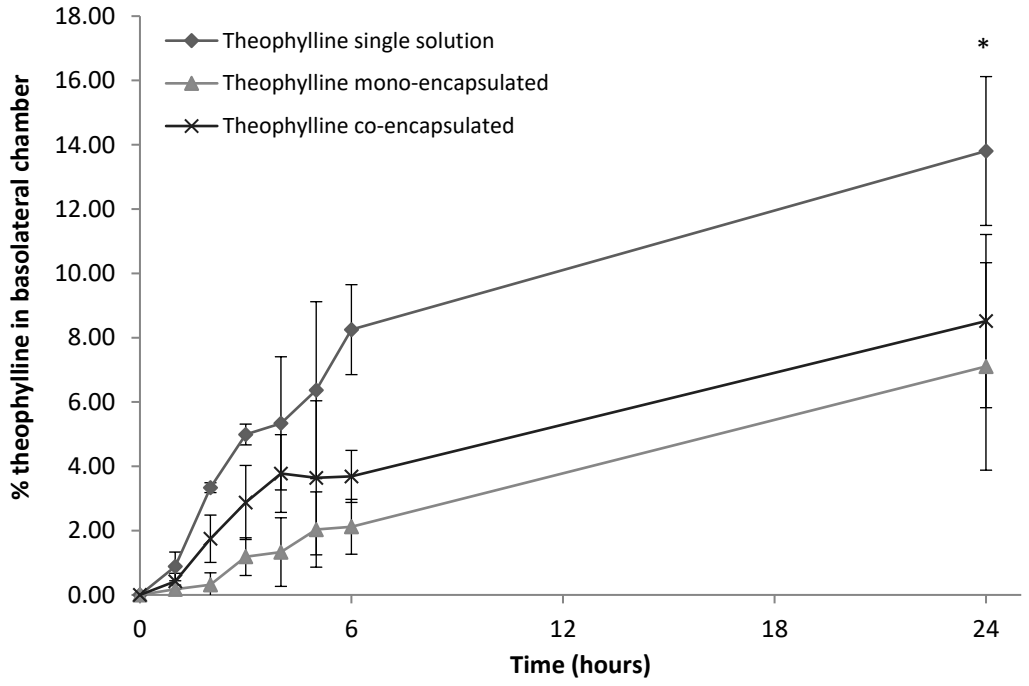


930

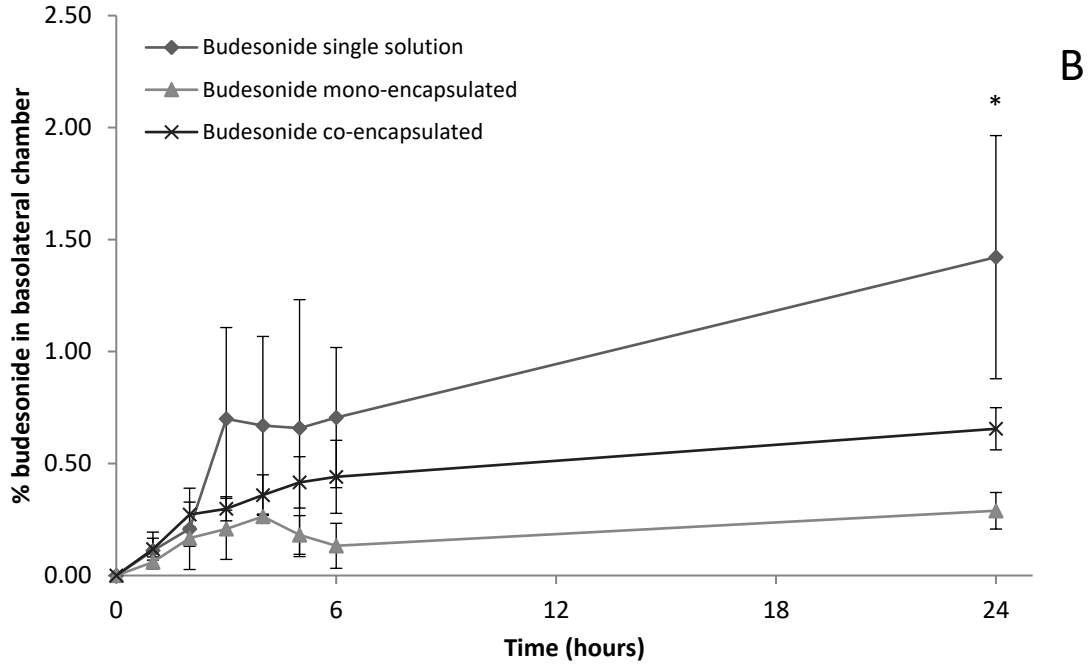


**Figure 7**

935

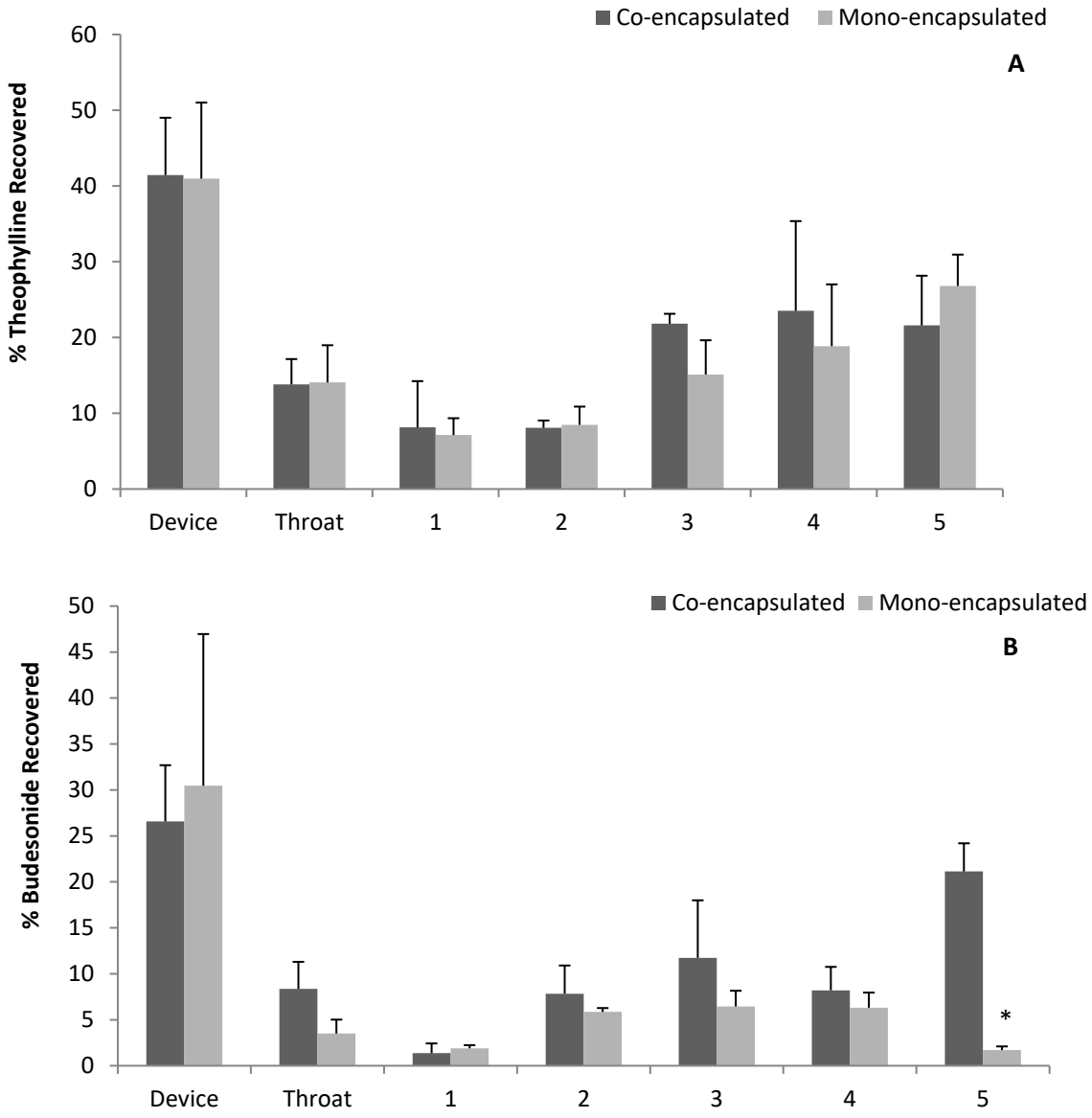
Co-encapsulated
Mono-encapsulated
A
% Theophylline Recovered
60
50
40
30
20
10
0
Device
Throat
1
2
3
4
5
Co-encapsulated
Mono-encapsulated
B
% Budesonide Recovered
50
45
40
35
30
25
20
15
10
5
0
*
Device
Throat
1
2
3
4
5

**Figure 8**

940

**Table captions**

**Table 1:** Preparation and characterization of PLA nanoparticles. The aqueous phase consisted of theophylline (50 mg) dissolved in 2% w/v PLA. Budesonide (5 mg) and PLA (200 mg or *50 mg) dissolved in dichloromethane. Average particle size (nm) and average zeta potential (mV) of mono- and co-encapsulated nanoparticles compared to blank PLA nanoparticles (n=3, mean ± SD). Average loading efficiency of theophylline and budesonide measured using HPLC was obtained for mono-encapsulated and co-encapsulated PLA nanoparticles using blank PLA nanoparticles as controls (n=3, mean ± SD)

**Table 2:** The effect of blank nanoparticles, solutions of theophylline and budesonide and mono- and co-encapsulated theophylline and budesonide on the apparent permeability of FD4 across 16HBE14o- cells. (n=3; blank nanoparticles or 9 remaining studies, mean ± SD)

**Table 3:** The apparent permeability coefficients of theophylline and budesonide across the 16HBE14o- cells from solution and mono- and co-encapsulated nanoparticles (n=9, mean ± SD) (*$P$<0.05 for single and combined counterparts – solutions and nanoparticles).

**Table 1**

| Method Number | 2nd organic solvent | Volume of excess aqueous phase (ml) | Removal of organic solvent (rotary evaporation, mbar OR overnight stirring, rpm) | Mean particle size ± SD (nm) | Mean zeta potential ± SD (mV) | Loading efficiency ± SD (%) | |
|---|---|---|---|---|---|---|---|
| | | | | | | Theophylline | Budesonide |
| ***Co-encapsulated Nanoparticle preparation*** | | | | | | | |
| 1 | – | 100 | 100 mbar | 278.89±35.67 | -16.90±5.77 | 9.62±5.37 | 48.20±27.57 |
| 2 | Acetone | 100 | 100 rpm | 483.48±184.46 | -12.35±6.30 | 1.16±1.12 | 9.88±1.76 |
| 3 | Acetone | 50 | 100 rpm | 139.13±45.62 | -0.88±3.35 | 13.45±3.03 | 39.92±4.59 |
| 4* | Acetone | 50 | 100 rpm | 473.47±153.74 | -20.58±4.02 | 1.27±0.07 | 3.75±0.27 |
| 5 | Acetone | 100 | 254 mbar | 243.80±26.28 | -8.01±4.16 | 2.55±0.09 | 8.23±2.97 |
| 6 | Acetone | 100 | 44 mbar | 230.18±25.57 | -20.92±19.73 | 0.03±0.01 | 0.11±0.06 |
| 7 | Ethyl acetate | 100 | 100 mbar | 186.09±17.27 | -20.33±7.10 | 20.70±5.67 | 28.39±8.28 |
| 8 | Acetone | 100 | 70 mbar | 216.71±14.90 | -19.26±6.50 | 17.79±5.59 | 29.84±1.47 |
| 9 | Acetonitrile | 100 | 80 mbar | 191.56±21.99 | -13.55±5.63 | 29.43±4.90 | 35.09±3.65 |
| ***Mono-encapsulated Nanoparticle preparation using method 8*** | | | | | | | |
| Blank NP | Acetone | 100 | 70 mbar | 337.23±71.63 | -16.61±1.00 | – | – |
| Theophylline NP | Acetone | 100 | 70 mbar | 418.78±81.70 | -16.22±0.56 | 18.86±5.28 | – |
| Budesonide NP | Acetone | 100 | 70 mbar | 192.30±63.19 | -13.17±1.11 | – | 39.17±18.39 |

965

**Table 2:**

| Time period | 0-6 hours | 6-24 hours | 0-24 hours |
|---|---|---|---|
| | **Papp ($x10^{-6}$cm/s)** | **Papp ($x10^{-6}$cm/s)** | **Papp ($x10^{-6}$cm/s)** |
| Control | 0.08±0.01 | 0.13±0.01 | 0.12±0.01 |
| Blank PLA NPs | 0.09±0.01 | 0.13±0.00 | 0.12±0.00 |
| | | | |
| Control | 0.13±0.02 | 0.19±0.01 | 0.18±0.01 |
| Theophylline solution | 0.12±0.03 | 0.17±0.01 | 0.16±0.01 |
| Budesonide solution | 0.19±0.01 | 0.15±0.00 | 0.15±0.01 |
| | | | |
| Control | 0.09±0.01 | 0.15±0.01 | 0.14±0.01 |
| Mono-encapsulated theophylline | 0.08±0.01 | 0.18±0.03 | 0.16±0.02 |
| Mono-encapsulated budesonide | 0.09±0.02 | 0.17±0.03 | 0.16±0.03 |
| Co-encapsulated theophylline & budesonide | 0.10±0.02 | 0.16±0.03 | 0.15±0.02 |

970 **Table 3:**

| Time period | 0-6 hours | 6-24 hours | 0-24 hours |
|---|---|---|---|
| | **Papp ($x10^{-6}$ cm/s)** | **Papp ($x10^{-6}$ cm/s)** | **Papp ($x10^{-6}$ cm/s)** |
| Theophylline solution | 3.49±0.51* | 0.78±0.13 | 1.29±0.23 |
| Mono-encapsulated theophylline | 0.97±0.46 | 0.54±0.33 | 0.61±0.33 |
| Co-encapsulated theophylline | 1.45±0.74 | 0.82±0.23 | 0.81±0.23 |
| Budesonide solution | 0.19±0.10 | 0.10±0.03 | 0.12±0.05 |
| Mono-encapsulated budesonide | 0.03±0.03 | 0.01±0.00 | 0.02±0.01 |
| Co-encapsulated budesonide | 0.15±0.04* | 0.02±0.00 | 0.05±0.00 |